Environ. Sci. Technol. **2004**, *38,* 2792−2801

Zn Speciation in the Organic Horizon of a Contaminated Soil by Micro-X-ray Fluorescence, Micro- and Powder-EXAFS Spectroscopy, and Isotopic Dilution

GÉRALDINE SARRET,*,† JÉROME BALESDENT,‡ LAMIA BOUZIRI,‡ JEAN-MARIE GARNIER,§ MATTHEW A. MARCUS,|| NICOLAS GEOFFROY,† FRÉDÉRIC PANFILI,† AND ALAIN MANCEAU†

Environmental Geochemistry Group, LGIT, University of Grenoble and CNRS, BP 53, 38041 Grenoble, Cedex 9, France, Laboratoire d'Ecologie Microbienne de la Rhizosphere, UMR CNRS/CEA, no. 163 CEA DEVM Centre de Cadarache, 13108 Saint-Paul lez Durance, Cedex, France, Universite Aix Marseille 3, CNRS, CEREGE, 13545 Aix en Provence, France, and Lawrence Berkeley National Laboratory, Advanced Light Source, MS 6-2100, Berkeley, California 94720

Soils that have been acutely contaminated by heavy metals show distinct characteristics, such as colonization by metal-tolerant plant species and topsoil enrichment in weakly degraded plant debris, because biodegradation processes are strongly inhibited by contamination. Such an organic topsoil, located downwind of an active zinc smelter and extremely rich in Zn (∼2%, dry weight), was investigated by X-ray diffraction, synchrotron-based X-ray microfluorescence, and powder- and micro-extended X-ray absorption fine structure (EXAFS) spectroscopy for Zn speciation and by isotopic dilution for Zn lability. EXAFS spectra recorded on size fractions and on selected spots of thin sections were analyzed by principal component analysis and linear combination fits. Although Zn primary minerals (franklinite, sphalerite, and willemite) are still present (∼15% of total Zn) in the bulk soil, Zn was found to be predominantly speciated as Zn−organic matter complexes (∼45%), outer-sphere complexes (∼20%), Zn-sorbed phosphate (∼10%), and Zn-sorbed iron oxyhydroxides (∼10%). The bioaccumulated Zn fraction is likely complexed to soil organic matter after the plants' death. The proportion of labile Zn ranges from 54 to 92%, depending on the soil fraction, in agreement with the high proportion of organically bound Zn. Despite its marked lability, Zn seems to be retained in the topsoil thanks to the huge content of organic matter, which confers to this horizon a high sorption capacity. The speciation of Zn in this organic soil horizon is compared with that found in other types of soils.

* Corresponding author phone: +33 (0)4 76 82 80 21; fax: +33 (0)4 76 82 81 01; e-mail: gsarret@ujf-grenoble.fr.
† University of Grenoble and CNRS.
‡ UMR CNRS/CEA.
§ CEREGE.
|| Lawrence Berkeley National Laboratory.

Introduction

Atmospheric emissions from nonferrous metal industries generate extended diffuse contamination as well as acute contamination of the local environment (*1*). Since smelting facilities were historically located in densely populated areas, there is a risk of metal ingestion by humans, essentially by inhalation of dust particles and also via the transfer of metals to the drinking water and to the food chain. The zinc smelter of Auby (Nord, France) has been operating since 1869 and produces ca. 230 000 t of Zn annually. The surrounding soils are strongly contaminated with Zn, Pb, and Cd, as shown by several studies conducted in this area (*2*−*5*). Near the smelter, a particular ecosystem composed of Zn-hyperaccumulating (*Arabidopsis halleri* and *Viola calaminaria*) and Zn-tolerant plants (*Populus* sp., *Armeria maritima*, *Arrhenaterum elatius*, and *Silene vulgaris*) has developed. Zinc contamination is restricted to the top layer of the soil (*3*), which consists mainly of partially decomposed plant fragments and organic matter resulting from the inhibition of biodegradation processes due to metal toxicity (*5*). Similar organic layers have been reported in many other contaminated sites (*6*−*8*). The hyperaccumulation of metals in plant tissues, leading to the enrichment in metals of the topsoil after several vegetative cycles, has been proposed as a type of allelopathy, which would create toxic conditions for nontolerant species (*9*, *10*). The most common mechanism of Zn storage in hyperaccumulating plants is their sequestration in vacuoles as organic acid complexes (*11*−*14*). However, the fate of these metals after the plants' death is unknown. The purpose of this study is 3-fold: (i) to identify and quantify the chemical forms of Zn in a topsoil rich in plant debris and residual organic matter near the Auby smelter, which is a generic case for this kind of contamination; (ii) to estimate the bioavailability of Zn in this particular ecosystem; and (iii) to evaluate the fate of bioaccumulated Zn after plants' death.

EXAFS (extended X-ray absorption fine structure) spectroscopy is a tool of choice for probing the local environment of Zn in soils and sediments (*8*, *15*−*19*). This method is sensitive to metals included in mineral structures, to metal precipitates, and sometimes to inner-sphere mineral surface complexes. It is less sensitive to metals bound to matrixes composed of light elements such as organic matter and to metals present as outer-sphere surface complexes. In natural systems, all these species may be present altogether, and the EXAFS signal from organic and outer-sphere complexes is then masked by the more intense signal from other species. To obtain the EXAFS spectra of pure species, one can combine powder-EXAFS on bulk sample with chemical treatments (*8*, *17*, *19*) or use micro-focused EXAFS (μEXAFS) spectroscopy (*16*, *18*, *20*−*22*). In practice, however, most natural systems are still heterogeneous at the micrometer-scale, and μEXAFS spectra may be a weighted sum of component spectra from several individual species. Since the proportions of metal species are different in the bulk and in the set of laterally resolved EXAFS spectra, their number and nature can be obtained by principal component analysis (PCA) (*8*, *17*, *21*, *23*, *24*). Eventually, the proportion of each species in the whole soil matrix is determined by decomposing the bulk average EXAFS spectrum with a linear combination of reference spectra identified by PCA.

The proportion of labile metal species can be estimated by chemical techniques, such as $CaCl_2$ extraction (*25*) and isotopic dilution (*26*−*28*). This pool is operationally defined by its exchangeability between the solid phase and the solution during a given time. Most labile species consists of outer-sphere and weakly bound inner-sphere complexes on

10.1021/es035171t CCC: $27.50
Published on Web 04/13/2004

mineral surfaces and organic matter. In this study, physical techniques including X-ray diffraction (XRD), synchrotron-based X-ray microfluorescence (μSXRF), and powder-EXAFS and μEXAFS spectroscopy were combined with isotopic dilution to obtain an in-depth description of the nature and proportion of the labile and nonlabile Zn species present in the studied organic soil.

Materials and Methods

Site and Soil Description. The soil studied comes from the Bois des Asturies in Auby (Nord, France), a poplar plantation located near and downwind an operating zinc smelter. The soil profile, its humus morphology, and floral and faunal composition were described by Gillet and Ponge (*5*). The soil presents a thick holorganic (i.e., essentially organic) OM horizon made of weakly degraded plant litter and roots, similar to a peat but with almost neutral pH (6.2). This layer is characterized by an extremely high Zn content (more than 2% dry weight). The changes in vegetation cover have been traced over recent decades based on the identification of plant siliquae. The ground was covered by mosses before the colonization by *A. halleri* and a more recent additional colonization by *V. calaminaria*. Animal feces are almost absent throughout the organic horizon. The preservation of organic matter is believed to result from the resistance of metal-rich plant debris to microbial attack and from the low faunal activity combined with an avoidance behavior of saprophagous fauna; for instance, Collembola found in the soil feed either on aerial deposits (spores, pollens) or on the underlying substrate (silt and clay particles and their attached microflora) (*5*).

In one of the most polluted zones, referred to as P2 in Gillet and Ponge (*5*), blocks of 550 cm^2 horizontal $\times$ 12 cm vertical ($H \times V$) were extracted from the field in triplicate. The thick holorganic horizon was separated in two layers called O1 (0−7 cm) and O2 (7−12 cm). The underlying A horizon contains much less organic carbon (TOC <20 mg g^{-1} as compared to ~380 mg g^{-1} in the topsoil, as determined by elemental analyzer) and zinc (<2000 g kg^{-1} as compared to about 2% in the topsoil, as determined by inductively coupled plasma−atomic emission spectrometry (ICP−AES)). The present study is focused on the O2 layer. Soil samples were dried at 50 °C, weighted, and sieved at 2 mm. Particle-size and density fractions were separated after mechanical dispersion according to Balesdent et al. (*29*). Briefly, 75 g of dry soil (<2 mm) was placed in a 1-L polypropylene flask with 40 g of 5 mm diameter glass beads and 750 mL of deionized water and then shaken for 16 h in a rotating shaker at 60 rpm. The 50−200, 200−500, and 500−2000 μm particle-size fractions were separated by wet sieving. To limit the leaching of Zn during sieving, the water was recycled during the fractionation process. From the >50 μm fractions, low-density organic debris (fraction L) were separated from higher density mineral material (fraction H) by repeated differential sedimentation in water. The H component was absent from the 500−2000 μm fraction and not separated from the 0−50 μm fraction. The final 0−50 μm suspension (2 L) was centrifuged at 7000*g*. The dissolved organic carbon in the supernatant was 1.3 mg g^{-1} of soil as compared to ~380 mg g^{-1} for TOC.

Labile Zn was determined by isotopic dilution in the 0−50, 50−200, and 200−500 μm fractions. The soil samples were homogenized, and four replicates of 200 mg were added to 60 mL of $Ca(NO_3)_2$ 10^{-3} M and immediately spiked with 60 μL of acidic ^{65}Zn solution containing 5.8×10^{-10} g/L of ^{65}Zn and 1.3×10^{-7} g/L of stable Zn. The pH of the suspension was adjusted (±0.2) close to the initial pH of the suspension (6.2). All samples were shaken for 48 h at 25 °C and then filtered with 0.2-μm Nucleopore filters. A 76-h kinetic study showed that steady state of the concentrations in solution was reached after 24 h. Concentration of stable Zn in the filtrate was measured by ICP−AES, and labeled Zn concentration was measured by γ-spectrometry using a Ge coaxial detector (Eurysis Mesures). The isotopically exchangeable Zn content (E value, g of Zn kg^{-1}) is the quantity of Zn in the soil with the same liquid/solid ratio as the ^{65}Zn:

$$E_{Zn} = [Zn]_{sol}(*K_d + L/S) \quad (1)$$

where $[Zn]_{sol}$ is the concentration of Zn in solution (g L^{-1}), $*K_d$ is the solid/liquid concentration of radioactive Zn (L kg^{-1}), and L/S is the liquid-to-solid ratio (L kg^{-1}) (*26*−*28*). The relative proportion of isotopically exchangeable Zn to aqua regia soluble Zn (% E) is defined as

$$\% E = (E_{Zn}/[Zn]_T) \times 100 \quad (2)$$

where $[Zn]_T$ is the aqua regia soluble Zn content (g kg^{-1}).

X-ray Diffraction. XRD patterns were recorded on powders with a Siemens D501 powder diffractometer equipped with a scintillation detector using Co Kα radiation (40 kV and 37.5 mA). Intensities were measured at intervals of 0.04° 2θ with a 10-s dwell time per point.

Powder EXAFS. Powder Zn K-edge EXAFS spectra were measured at room temperature on beamline D42 at the Laboratoire du Rayonnement Electromagnétique (LURE, Orsay, France) in transmission mode using ionization chambers for Zn-rich samples and on beamline FAME at the European Synchrotron Radiation Facility (ESRF, Grenoble, France) in fluorescence mode using a 30-element solid-state Ge detector (Canberra) for the least concentrated samples ([Zn] < 10 000 mg kg^{-1}). The spectra presented are the sum of 2−4 scans of about 40 min each, depending on Zn concentration.

***μ*SXRF and *μ*EXAFS.** μSXRF and μEXAFS measurements were performed on beamline 10.3.2 at the Advanced Light Source (ALS, Berkeley, CA), operating at 1.9 GeV and 200−400 mA. Particles from the H50−200 and 500−2000 μm fractions were embedded in epoxy resin and prepared as 30-μm-thick thin sections. The thin sections were mounted on a $x-y$ translation stage, the incident beam intensity (I_0) was measured using an ionization chamber, and the fluorescence yield was measured using a seven-element Ge solid-state detector. For μSXRF measurements, the incident beam energy was 9.7 keV, the beam size and pixel size were 10 μm (H) × 5 μm (V), and the dwell time was 100 ms $pixel^{-1}$. The fluorescence yield was normalized by I_0 and the dwell time. μEXAFS spectra were recorded on selected regions of the samples on the basis on elemental associations obtained from μSXRF maps. For μEXAFS measurements, the spot size was 15 μm (H) × 5 μm (V). The spectra presented are the sum of 2−12 scans of about 40 min each, depending on Zn concentration in the region probed.

EXAFS Data Analysis. Powder EXAFS and μEXAFS spectra were normalized following standard methods. Data analysis was performed by combining PCA with linear combination fits (LCFs). The PCA and the LCF procedures used here were described previously (*17*, *21*, *30*). For this approach, an extensive library of Zn model compounds was used (see Results and Discussion). Zinc citrate was purchased from Alfa. The preparation of zinc malate and Zn-sorbed ferrihydrite ($5Fe_2O_3 \cdot 0.9H_2O$) (ZnFh) containing 1500 mg kg^{-1} Zn were described previously (*16*, *30*). Zn-sorbed apatite was prepared under Ar atmosphere by slowly adding a Zn nitrate solution at pH 5 to a synthetic apatite suspension ($Ca_5(PO4)_3(OH)_2$, purchased from Brenntag, Germany), the pH being maintained at 5.0. After 24 h of equilibration, the suspension

TABLE 1. Elemental Concentrations of the Soil Fractions[a]

soil fraction	wt (g g^{-1})	organics (mg g^{-1})						metals (mg kg^{-1})				major elements (%)					
		C	N	C/N	P	S	C/S	Zn	Pb	Cd	Cu	SiO_2	Al_2O_3	Fe_2O_3	CaO	MnO	H_2O
500−2000 μm	0.072	421	26	16	2.0	2.0	211	19538	1600	135	420	5.82	1.10	1.12	1.30	0.12	85.96
L200−500 μm	0.073	424	28	15	2.0	2.4	177	17542	6080	178	431	7.72	1.54	1.36	1.40	0.08	82.80
H200−500 μm	0.016	116	3	39	0.6	2.0	58	1542	480	18	66	68.86	3.72	1.52	0.98	0.02	23.36
L50−200 μm	0.212	458	20	23	2.0	2.0	229	10176	6250	224	350	12.82	4.44	2.08	1.36	0.08	74.60
H50−200 μm	0.087	524	3	175	0.9	5.6	94	9432	4825	116	240	31.08	8.46	4.04	1.40	0.10	50.18
0−50 μm	0.540	288	1	288	3.3	6.9	42	19740	8550	231	460	28.46	8.00	6.42	1.68	0.16	47.02
bulk (calcd)	1.0	361	9	40	2.6	5.0	72	16354	6931	205	406	22.86	6.25	4.46	1.53	0.13	58.19
bulk before fractionation (measd)		376	18	21	2.0	6.6	57	21078	9135	270	406	23.42	5.72	4.60	1.66	0.12	59.14

[a] Concentrations in C, N, P, and S were determined with an elemental analyzer. Concentrations in metals and major elements were determined by digesting the soil samples in aqua regia and analyzing the solutions by inductively coupled plasma−atomic emission spectrometry (ICP−AES).

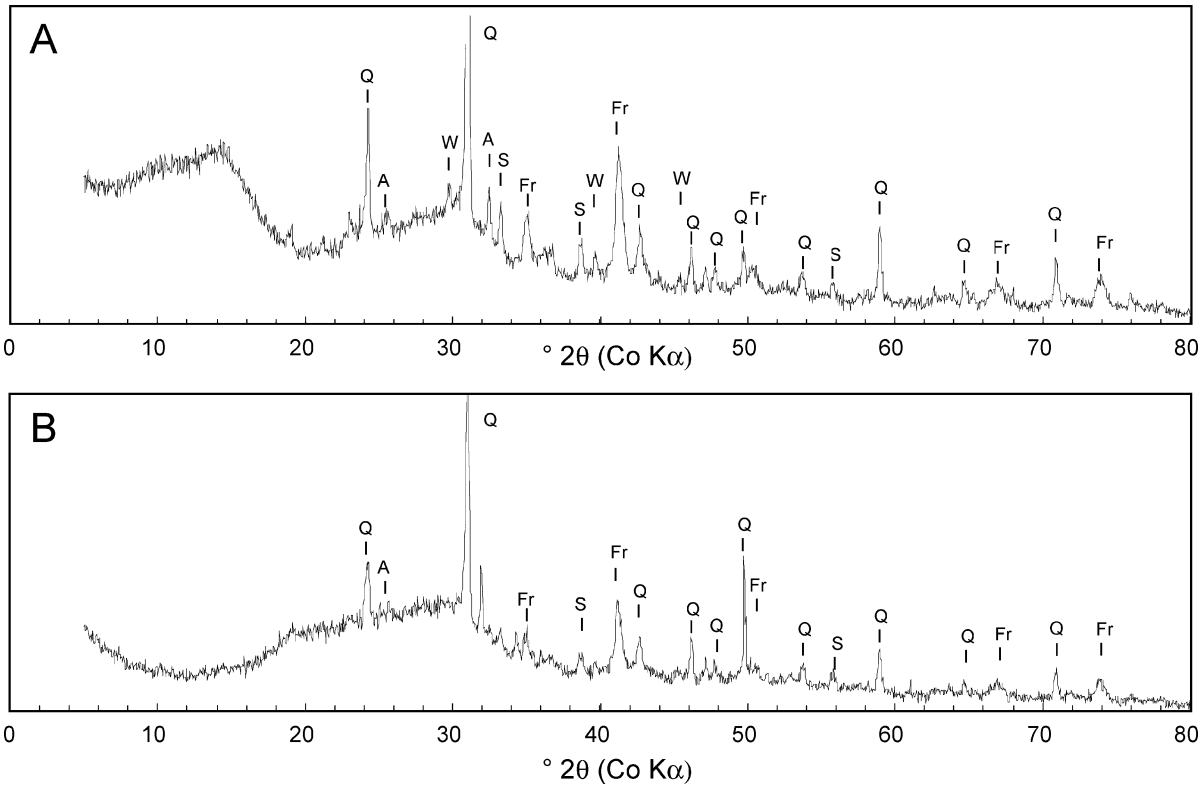

FIGURE 1. XRD pattern for the <50 μm fraction (A) and the bulk soil (B). Minerals identified are quartz (Q), franklinite (Fr), willemite (W), sphalerite (S), and anorthite (A).

was centrifuged and freeze-dried. Zn concentration in the solid phase was 1% weight. Zinc phytate spectrum was provided by J. Cotter-Howells (University of Aberdeen, Scotland).

Results and Discussion

The soil material is characterized by a high content of organic carbon (~38%, Table 1). This organic matter is mostly present in the coarse fraction (half of it was found in the >50 μm fraction), indicating a low degree of degradation. The H fractions account for about 10% of the soil and contain quartz sand, primary minerals, and a black carbonaceous material, probably coal used by the smelter. Analysis of this coal showed a high C/N ratio (150) and a low C/S ratio (15−20). The C/N ratio higher than 20 and the C/S ratio lower than 100 for the 0−50 μm, H50−200, and H200−500 μm fractions denote the presence of coal. The fact that the 0−50 μm fraction has a higher C/N value (288) than the coal (150) probably arises from an underestimation of N content in this sample (1 mg g^{-1}). The P content of the soil (2000 mg kg^{-1}) is relatively high as compared to typical values reported for soils under temperate climate (between 100 and 3000 mg kg^{-1}; *31*). The high P content suggests that this soil has been used for agriculture in the past.

Zn concentrations are high in all fractions (between 9432 and 19740 mg kg^{-1}) except in the H200−500 μm fraction (1542 mg kg^{-1}). The soil also contains significant amounts of Pb, Cd, and Cu. Metal concentrations calculated from the weight and analysis of the fractions are lower than those measured on the soil before fractionation, which indicates that metals were partly leached out during the fractionation process. Some Zn-bearing minerals were detected by XRD (Figure 1, Table 2). Franklinite ($ZnFe_2O_4$) and sphalerite (ZnS) were identified in all fractions but H200−500 μm, which is mostly composed of quartz and contains only ~1540 mg kg^{-1} Zn. Willemite (Zn_2SiO_4) was detected in the H50−200 and 0−50 μm fractions. Sphalerite probably originates from the Zn ore used in the smelter, whereas franklinite, willemite, and mullite ($Al_6Si_2O_{13}$) are high-temperature minerals probably formed during the smelting process.

TABLE 2. Minerals Identified by XRD

soil fraction (μm)	quartz SiO_2	franklinite $ZnFe_2O_4$	sphalerite ZnS	willemite Zn_2SiO_4	anorthite $CaAl_2Si_2O_8$	mullite $Al_6Si_2O_{13}$
500−2000	+	+	+			
L200−500	+	+	+			
H200−500	+ + +					
L50−200	+	+	+			
H50−200	+ +	+	+	+		+
0−50	+ +	+	+	+	+	
bulk soil	+	+	+		+	

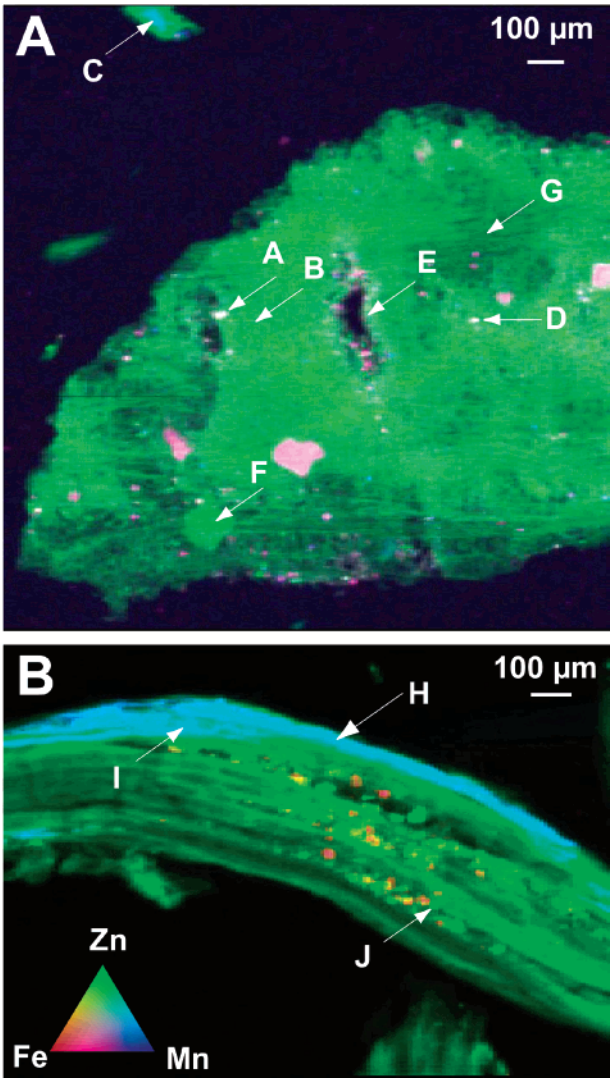

FIGURE 2. μSXRF elemental maps for organic fragments of the 500−2000 μm fraction. Ratio of maximal counts: 11 for Zn Kα/Fe Kβ and 34 for Zn Kα/Mn Kα (A), 7 for Zn Kα/Fe Kβ and 6 for Zn Kα/Mn Kα (B).

The μSXRF elemental maps for particles of the 500−2000 μm fraction (Figure 2) suggest two major Zn pools. The first pool is composed of diffuse and rather homogeneous Zn areas, in which Zn is probably associated with organic matter. In the Figure 2B, Zn distribution shows a fibrous appearance that may correspond to cell walls of the partially decomposed plant tissue. The second pool consists of Zn-concentrated spots, which occasionally contain also Fe, Mn, Cu, or Cr (last two not shown). In the H50−200 μm fraction, Zn is also present in a variety of elemental associations (Figure 3). On the basis of the nature of Zn minerals identified by XRD, the bright green particles (i.e., where Zn is predominant) can be tentatively attributed to sphalerite or willemite, and the mixed

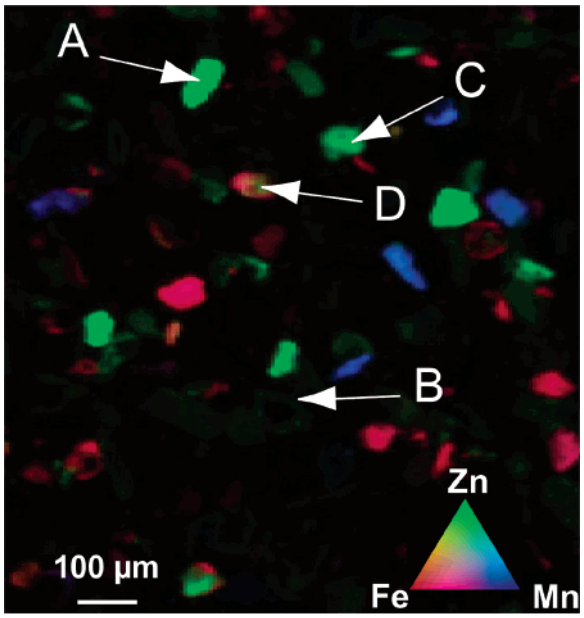

FIGURE 3. μSXRF elemental map for the fraction H50−200 μm. Ratio of maximal counts: 10 for Zn Kα/Fe Kβ and 11 for Zn Kα/Mn Kα. Spot E was found in another region of the thin section (not shown).

TABLE 3. Output Parameters of the Principal Component Analysis

component	eigenvalue	IND[a]	total NSS[b] (%)
1	133.0	3.55×10^{-2}	18.62
2	47.0	2.72×10^{-2}	8.34
3	29.9	2.23×10^{-2}	4.32
4	15.9	2.20×10^{-2}	3.16
5	15.1	2.09×10^{-2}	2.11
6	10.7	2.13×10^{-2}	1.58
7	9.4	2.18×10^{-2}	1.18
8	7.3	2.34×10^{-2}	9.34

[a] Indicator value (*32*). [b] Total NSS $= \sum_{spectra}\sum_{i}[k^3\chi_{exp} - k^3\chi_{reconst}]^2 / \sum_{spectra}\sum_{i}[k^3\chi_{exp}]^2 \times 100$.

green and red particles (i.e., containing Zn and Fe) can be attributed to franklinite.

On the basis of these elemental distributions and associations, spots were selected and their μEXAFS spectra recorded. Bulk EXAFS spectra of the various fractions were recorded as well. The whole set of spectra and Fourier transforms are shown in Figure 4. The top spectra, with a high amplitude and clear multiple-shell contributions, are typical of mineral structure, whereas the bottom spectra suggest an organic environment for Zn. PCA was applied to the whole data set in order to evaluate the number of individual Zn species and to identify them. The output parameters, including the eigenvalues, the indicator values (IND), and the total normalized sum-squares residuals (total NSS) for the first eight components are given in Table 3, and the component spectra are shown in Figure 5. IND is supposed to be minimum when the number of principal components is reached (*32*). In this study, IND was minimum with five components (Table 3). However, Figure 5 shows that the fifth component contains very little signal but essentially noise. Moreover, the whole set of experimental spectra was reconstructed correctly with four components, and the quality of the reconstruction, evaluated by total NSS values and by visual inspection, did not improve significantly with five components (Table 3). Therefore, the system can be described with four independent components only. Then, the nature of Zn species was determined by target trans-

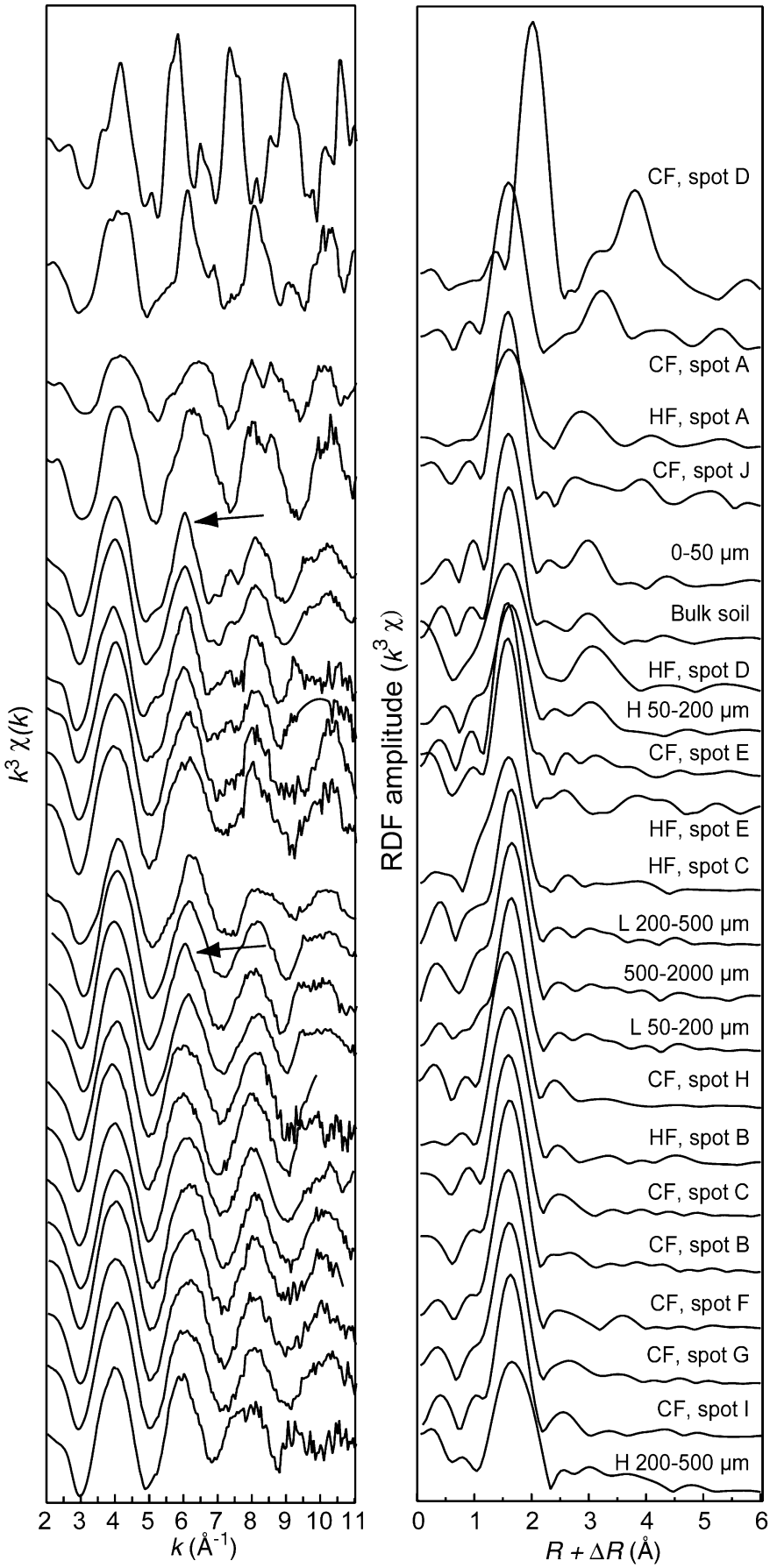

FIGURE 4. Zn K-edge EXAFS spectra and radial distribution functions (RDFs) for the soil samples. CF (coarse fraction): 500−2000 μm fraction; HF (heavy fraction): H50−200 μm fraction. The sharp-pointed oscillations indicated by the arrows are due to franklinite.

TABLE 4. Proportions (in % mole fraction) of Zn Species Determined by LCF

sample	franklinite	sphalerite	willemite	ZnFh	zinc phosphate	Zn−organic acids	sum	NSS[a] (%)
Soil Fractions (Powder EXAFS)								
bulk soil	9[b]	4[b]	0	10	11	64	98	4.1
500−2000	5[b]	4[b]	0	0	0	90	99	3.7
L200−500 μm	5[b]	3[b]	0	0	0	89	97	2.2
H200−500 μm	8	20	0	0	11	69	108	11.6
L50−200 μm	5[b]	3[b]	0	0	0	89	97	3.1
H50−200 μm	10[b]	6[b]	0[b]	10	10	56	92	8.6
0−50 μm	13[b]	6[6]	0[b]	13	0	58	90	8.3
Microanalyses (μEXAFS) 500−2000 μm								
spot A	21	0	0	0	59	17	97	9.8
spot B	0	0	11	0	47	49	107	3.2
spot C	3	0	0	0	39	61	103	5.9
spot D	0	114	0	0	0	0	114	9.4
spot E	9	8	18	0	21	53	109	8.0
spot F	0	0	0	12	25	67	104	2.0
spot G	0	0	0	11	41	54	106	2.1
spot H	0	0	0	12	20	65	97	16.8
spot I	0	0	0	10	41	51	102	3.8
spot J	0	0	69	0	17	10	96	4.6
H50−200 μm								
spot A	0	0	47	0	0	0	47[c]	5.8
spot B	0	0	0	11	15	79	105	7.2
spot C	6	0	12	10	54	0	82	6.3
spot D	16	3	0	0	11	66	96	15.0
spot E	0	0	16	0	37	56	109	7.8

[a] Residual between fit and experimental data: NSS $= \Sigma_i[k^3\chi_{exp} - k^3\chi_{reconst}]^2/\Sigma_i[k^3\chi_{exp}]^2 \times 100$. [b] Indicates that the mineral was identified by XRD in this sample. [c] This low percentage is probably due to overabsorption. The precision is estimated to ±3% of total Zn for franklinite and sphalerite, and to ±10−20% (depending on the amplitude and shape of the reference spectra used) for other Zn species.

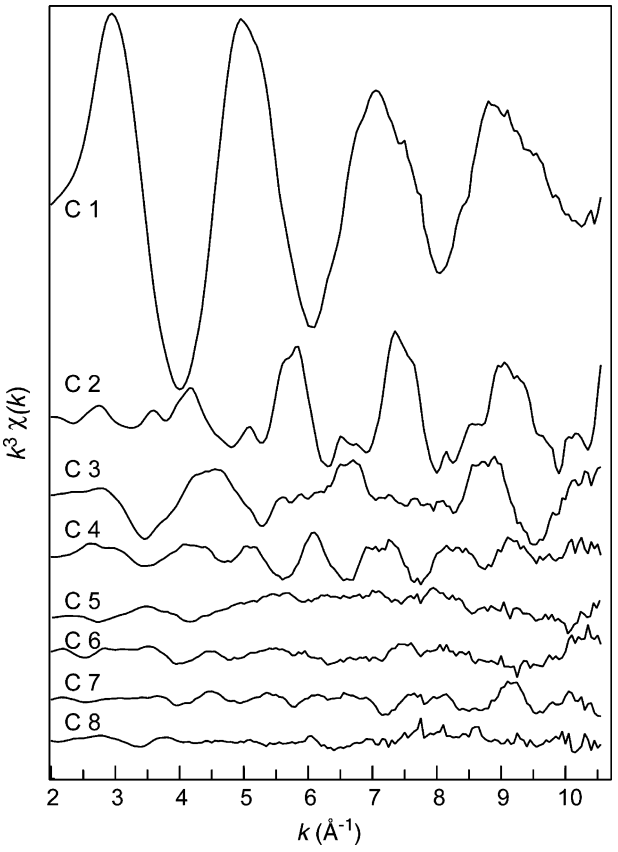

FIGURE 5. First (C1) to eighth (C8) component determined by principal component analysis of the whole set of EXAFS spectra shown in Figure 4.

formation (*32*) using an extensive library of mineral and organic Zn compounds, including Zn primary minerals, zinc phosphates, zinc carbonates, Zn sorbed on various minerals at different surface loadings and pH conditions as inner- and outer-sphere surface complexes, Zn complexed to organic acids, amino acids, humic and fulvic acids, fungi cell walls, and aqueous Zn (*30*, *33*, *34*). The quality of the transformation was evaluated by the normalized sum-squares (NSS) residual (Figure 6). Franklinite, sphalerite, willemite, and Zn-sorbed ferrihydrite (ZnFh) were positively identified by this analysis (Figure 6A). The reconstruction of the franklinite spectrum is not excellent because this species is never abundant in any sample, as shown below. An organic form and a mineral form of zinc phosphate (zinc phytate, myoinositol *kis*-hexaphosphate, and Zn-sorbed apatite, respectively) yielded satisfactory fits too. Other zinc phosphates, including hopeite, parahopeite, and zinc phosphate dihydrate, gave poor reconstructions (Figure 6B). A number of Zn species previously identified or inferred in soils and sediments, including zinc phyllosilicate (*8*, *16*, *17*, *19*, *22*, *34*), zinc hydrotalcite (*19*), Zn-sorbed birnessite (*16*, *34*), and outer-sphere Zn (*8*, *19*) (tested using aqueous Zn), also resulted in poor reconstructions, which indicates that these species are not present in significant amount in our soil. Of the Zn−organic compounds tested, the EXAFS spectra for a Zn−humic acid complex and for two Zn−organic acid complexes, Zn−malate and Zn−citrate, were satisfactorily reproduced but not those from Zn complexed to other organic acids (acetate, benzoate, formate, lactate, malonate, oxalate, and salicylate) nor to amino acids (aspartate, cysteine, glycine, and histidine), as illustrated in Figure 6B with oxalate and cysteine. The identification by EXAFS of the three primary minerals (franklinite, sphalerite, and willemite) is consistent with XRD results. Zn-sorbed iron oxyhydroxides, mimicked by ZnFh in this study, have been found in similar environmental contexts and probably result from the oxidation of sphalerite and pyrite (*15*, *17*). Since the spectra of the two phosphates look similar (Figure 6A), it is impossible to differentiate them conclusively. The generic term "zinc phosphate" is used thereafter for this pool. The inferred occurrence of Zn−malate and Zn−citrate was tested by

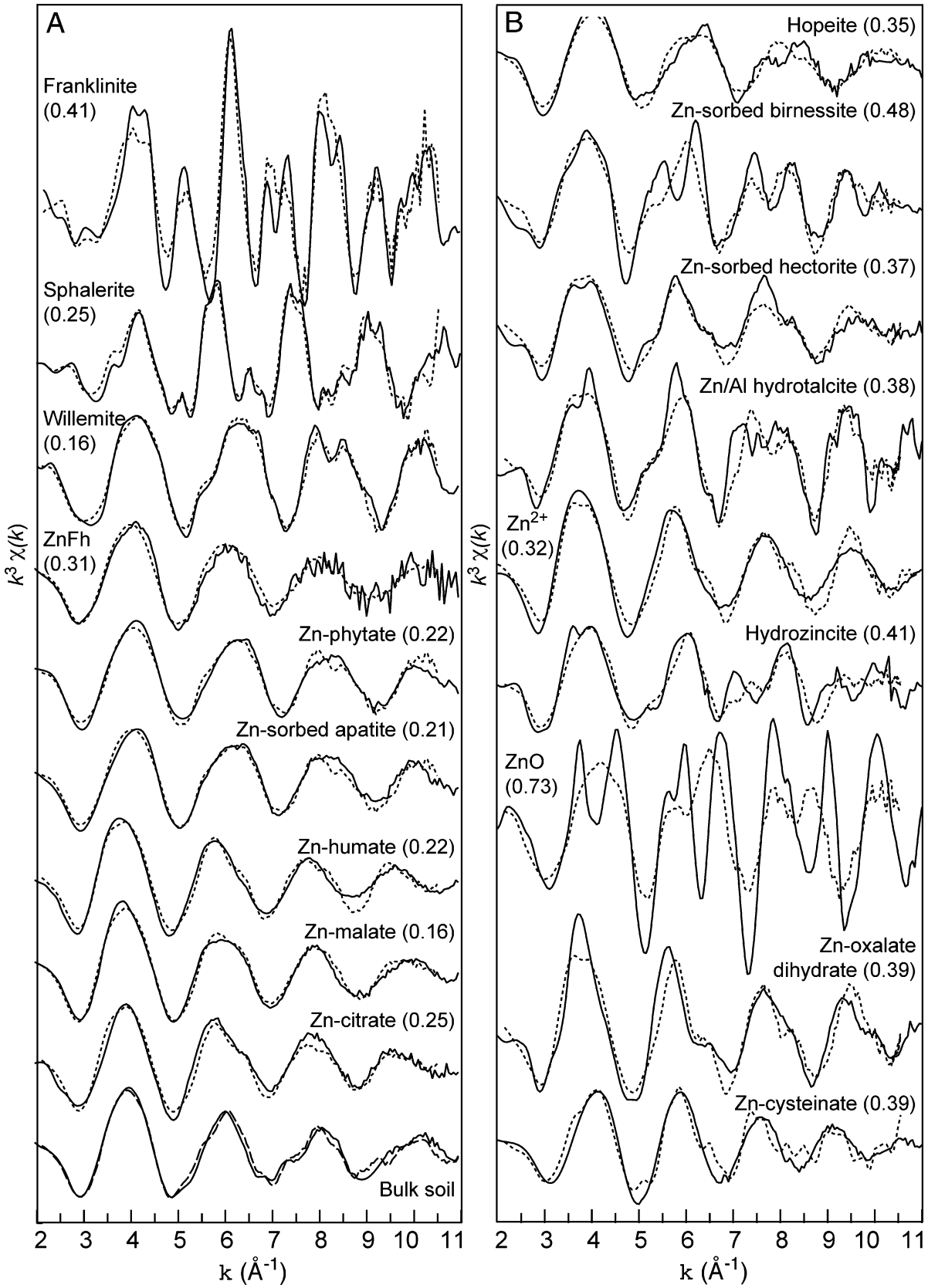

FIGURE 6. Zn K-edge EXAFS spectra (plain lines) and successful (A) and unsuccessful (B) target reconstructions (dotted lines) for reference compounds. The quality of the reconstruction is evaluated by the normalized sum-squares residuals, NSS $= \sum_i [k^3\chi_{exp} - k^3\chi_{reconst}]^2 / \sum_i [k^3\chi_{exp}]^2$ $\times$ **100, indicated in parentheses. The bottom spectrum in panel A shows the linear combination fit (dashed line) for the bulk soil (the proportion of each component is given in Table 4).**

measuring the two organic acids by ionic chromatography. The analysis was negative, so it is concluded that the two references species account for the general class of Zn complexed to various carboxyl and hydroxyl (alcohol and phenol) functional groups contained in overwhelming amount in the soil organic matter (620−660 cmol of total acidity per

TABLE 5. Comparison of EXAFS and Isotopic Dilution Results

	Zn pools determined by EXAFS (%)[a]				isotopic dilution parameters		
soil fraction	Zn primary minerals	ZnFh	zinc phosphate	Zn−organic acids	K_d (L kg^{-1})	E (g kg^{-1})	%E (%)
0−50 μm	19	13	0	58	313 (20)	10.6 (0.0)	53.7 (0.3)
50−200 μm	10	3	3	79	385 (12)	13.8 (0.6)	77.4 (3.4)
200−500 μm	12	0	2	85	450 (20)	17.4 (0.2)	92.0 (1.2)

[a] Zn primary minerals is the sum of franklinite, sphalerite, and willemite. Percentages in the fractions 200−500 and 50−200 μm were calculated from the percentage in the H and L fractions (Table 4) and from the weight of each fraction (Table 1).

kg of humic acids in temperate neutral soils; *35*). This pool, which was also fingerprinted by the Zn−humic acid reference, is referred to as "Zn−organic acids" below.

The Zn species identified by target transformation include franklinite, sphalerite, willemite, Zn-sorbed ferrihydrite, zinc phosphate, and Zn−organic acids. Their number is higher than the number of principal components (4) determined by PCA. A possible reason for this disagreement could be the occurrence of "background species", whose fractional amounts in all soil samples and spots analyzed are about constant (*21*). Results reported below show that this could be the case for Zn-sorbed ferrihydrite, whose proportion varies from 0 to 13% only. Another possible explanation for this disagreement is the fact that some EXAFS spectra, for instance, zinc phosphate, Zn-sorbed ferrihydrite, and Zn−organic acids, have similar features, and consequently, they are not truly independent vectors. A difference between the number of principal components and metal species was reported previously (*8*, *17*, *21*). The next step of the analysis was the determination by LCF of the proportion of each Zn species or group of species in the various bulk samples and spots analyzed. Each experimental spectrum was least-squares simulated by a combination of one to six spectra from the six Zn species previously identified. A new component species was considered to be significantly present if the NSS value decreased by at least 10%. Franklinite and sphalerite were identified in all the soil fractions (Table 3). Willemite was found in some spots of the thin sections but not in the soil fractions. The sensitivity of EXAFS is high for franklinite and sphalerite because their spectra have a high amplitude and multiple frequencies due to the presence of well ordered coordination shells. For franklinite, the sharp oscillation at about 6 Å^{-1} (Figure 5) is a good indicator for this species, as the occurrence of a small proportion of this mineral (down to 5%) modifies the profile of the second oscillation, which becomes sharp-pointed (arrows in Figure 4). The sensitivity to species in which the Zn local environment is disordered and/or composed of light elements, such as ZnFh, zinc phosphate, and Zn bound to organics, is clearly poorer (estimated at 10−20% of total Zn depending on the particular species).

The EXAFS spectrum for the bulk soil before fractionation was simulated with a combination of ∼65% organic Zn, ∼15% primary species (franklinite and sphalerite), ∼10% Zn-sorbed phosphate, and ∼10% Zn-sorbed iron oxyhydroxides. Although outer-sphere Zn complexes were dismissed using aqueous Zn^{2+} as a model for this pool, their presence cannot be ruled out. The leaching of Zn during wet sieving supports this hypothesis. In a study of an acidic organic topsoil impacted by a Zn smelter (pH 3.2), Scheinost et al. (*8*) reported 14% of outer-sphere Zn in the untreated soil, whereas this species was absent in the residue after extraction with 1 M ammonium nitrate. In another study on a Zn-contaminated soil (pH 5.5), Juillot et al. (*19*) found that 12% of Zn was $CaCl_2$-exchangeable and concluded from EXAFS and chemical extraction data that outer-sphere Zn was present in this soil. In this study, the comparison of Zn contained in the bulk soil before fractionation and the weighted sum of Zn in the size fractions shows that ∼20% of Zn was leached during size fractionation (Table 1). Thus, the proportion of loosely bound outer-sphere Zn may account for at least 20% of total Zn. Since Zn−organic complexes and hydrated Zn have relatively similar EXAFS spectra, the pool of outer-sphere Zn was likely overlooked and included to the Zn organic pool. This hypothesis was tested by replacing the 65% organic Zn component by 45% organic Zn + 20% Zn^{2+} in the simulation of the bulk soil spectrum. The fit quality was poorer but still satisfactory (NSS = 6.9% vs 4.1% using 65% Zn−organic acids). Consequently, the Zn species distribution in the bulk soil is more likely ∼45% Zn−organic acid complexes, ∼20% outer-sphere Zn, ∼15% franklinite and sphalerite, ∼10% Zn-sorbed phosphate, and ∼10% Zn-sorbed iron oxyhydroxides. The amount of Zn phosphate (10% of total Zn, i.e., 3.5×10^{-2} mol of Zn (kg of soil)$^{-1}$) is in the same range as the measured organic P concentration (0.2% P, i.e., 3.2×10^{-2} mol of P_2O_5 (kg of soil)$^{-1}$).

The comparison of the elemental associations found by μSXRF and of the chemical forms of Zn obtained by EXAFS shows that sphalerite and willemite are present in spots containing large amounts of Zn but small amounts of other metals and that franklinite is present in regions wherever there is Zn and Fe, and in some cases Cu and Cr. In the regions containing both Mn and Zn, Zn sorbed on manganese(III,IV) oxides, such as birnessite, was expected but not encountered. The diffuse Zn matrix, which represents the major pool of Zn, consists of organic Zn with a minor proportion of zinc phosphate and Zn-sorbed ferrihydrite.

The humus horizon is composed of litter of hyperaccumulating plants (*A. halleri* and *V. calaminaria*), moss, and poplar (*5*). *A. halleri*, the most abundant species, is known to store metals in its aerial parts, specifically in the vacuoles of the mesophyll cells and in the trichomes (*36*, *37*). An EXAFS study showed that Zn is predominantly octahedrally coordinated and complexed to malate in the plant shoots, whereas it is distributed between Zn−malate, Zn−citrate, and zinc phosphate forms in the roots (*30*). The absence of Zn−malate and Zn−citrate in the soil suggests that these complexes are dissociated during the biodegradation of the plants. A study on the hyperaccumulator *Thlaspi caerulescens* showed that metals present in leaves are highly labile once the leaves are incorporated into the soil (*38*). This lability is consistent with the sequestration of Zn in vacuoles since the cytoplasmic and vacuolar contents are released when the plant tissues are degraded. The zinc phosphate pool may originate from the decay of roots and also from chemical precipitation of dissolved Zn and P.

The proportion of labile Zn (%E) was determined by isotopic dilution in three size fractions of the soil (Table 5). The %E values range between 53.7 ± 0.3% and 92.0 ± 1.2%, and the distribution coefficients of ^{65}Zn (*K_d) range between 313 ± 20 and 450 ± 20 L kg^{-1} (log *K_d between 2.49 and 2.65). For comparison, Degryse et al. (*25*) measured %E in 47 polluted soils from Europe and reported values between 5 and 68%, with a median %E value of 26%. Sauvé et al. (*39*) reported an average log K_d (K_d = ratio between total and dissolved metal) of 2.87 ± 0.4 at pH 6.2 in contaminated and

TABLE 6. Soil Characteristics and Nature and Proportion of Zn Species Identified by EXAFS Spectroscopy

type of soil	pH	TOC (g/kg)	Zn (mg/kg)	Fe (g/kg)	Mn (g/kg)	Zn species, by decreasing order of abundance	ref
High Organic Content							
organic soil, made of partially decomposed plant residues[a]	3.2	320	6200	33	1.5	~60% franklinite ~30% sphalerite ~10% aqueous or outer-sphere Zn	*8*
organic soil, made of partially decomposed plant residues[a]	3.2		6200			~60−70% franklinite ~30−40% sphalerite Zn adsorbed to iron and manganese oxyhydroxides as inner-sphere complexes	*18*
wooded pseudogley brown leached soil (luvisol redoxisol)	5.5	640	1380	12.8	0.4	~50−60% outer-sphere and/or inner-sphere complexes on organic matter or goethite Zn−Al hydrotalcite Zn in dioctahedral phyllosilicate (<25%)	*19*
organic soil, made of partially decomposed plant residues	6.2	376	21078	32.2	0.9	~45% Zn bound to organic matter ~20% outer-sphere Zn ~15% primary species (franklinite and sphalerite) ~10% zinc phosphate ~10% Zn sorbed on iron oxyhydroxides	this study
Low Organic Content							
skeletal silty loam[b]	3.9	50	3700	25	0.5	~55% outer-sphere Zn ~45% Zn in hydroxy-Al interlayers of phyllosilicate	*8*
stony loam[b]	3.9		890			Zn bound to Al groups Zn sorbed on iron oxyhydroxides outer-sphere Zn or organic matter-bound Zn species	*18*
acid sandy soil (Maatheide)[c]			59220			Zn-substituted phyllosilicate hemimorphite willemite Zn-sorbed birnessite	*16*
sandy horizon (Mortagne)[d]	6.5−7.5		353−1405	12.0−23.9	0.2−0.5	Zn-substituted phyllosilicate Zn-sorbed birnessite Zn sorbed on iron oxyhydroxides	*16*
tilled soil (Evin-Malmaison)[e]	5.6−6.7		2318			Zn-substituted phyllosilicate Zn sorbed on iron oxyhydroxides	*16*
tilled pseudogley brown leached soil (luvisol redoxisol)	7.5	150	571	10.5	0.4	Zn−Al hydrotalcite Zn in dioctahedral sheet of phyllosilicate (<35%) ~25% outer-sphere and/or inner-sphere complexes on organic matter or goethite	*19*
Fragipan (Btx) horizon	4.5−5.0	-	128	92.3	13.1	~80−90% Zn in octahedral sheet and in hydroxy-Al interlayers of phyllosilicate ~10−20% sphalerite, zincochromite, lithiophorite, Zn-sorbed ferrihydrite, and zinc phosphate	*22*

[a,b] Same soils. [c] <40 μm fraction. [d] <100 μm fraction of four soil samples taken at 8−110 mm depth. [e] <50 μm fraction.

uncontaminated soils. The $*K_d$ values determined in this study can be approximated to K_d since the concentration of ^{65}Zn in the solution is negligible as compared to its concentration in the solid phase. The high %*E* values and low $*K_d$ values of this soil compared to average soils indicate that Zn is highly labile. Zn present in primary minerals is clearly not labile. Zn bound to iron oxyhydroxides, phosphates, and organic matter likely occupies a range of low to high affinity sites and can be considered as partly labile. The stock of ZnFh and zinc phosphate (2−13% of total Zn depending on the sample, as estimated from EXAFS data) cannot explain alone the high %*E* values (54−92% of exchangeable Zn), whereas the percentage of organic Zn is in good agreement with %*E* values, with an error bar of about 10% only (58−85% depending on the sample, Table 5). Thus, both methods agree on the dominance of Zn bound to soil organic matter in a predominantly labile form. Despite this high lability, Zn does not seem to be very mobile in the field at the scale of the soil profile. Indeed, the total concentration of Zn remains extremely high in the topsoil, despite the reduction of Zn emission by the smelter in recent years, and is an order of magnitude lower in the underlying mineral horizon. The persistence of Zn in the topsoil can be explained by the overwhelming amount of organic matter conferring to the soil a high sorption capacity. This sorption capacity is thought to increase with time since the biomass production is not balanced by the biodegradation of plant debris. Hyperaccumulating plants may also favor the upward movement of zinc, but this transfer is probably marginal because these plants have a small biomass.

The speciation of Zn found in this holorganic soil horizon is compared in Table 6 to previous data reported in the literature on various types of soils. Outer-sphere and organic Zn species have been suggested to amount ~50−60% in an organic acidic soil (pH 5.5) (*19*) and otherwise are present in subordinate amount in soils dominated by mineral constituents. In these soils, a varieties of Zn-sorbed and Zn-substituted secondary species were identified, including

phyllosilicates, iron oxyhydroxides, manganese oxides, lithiophorite, hydrotalcite, and phosphate (*8*, *16*, *18*, *19*, *22*). On the basis of these results, Zn−organic complexes seem to prevail in highly organic soils at moderately acidic pH.

In summary, EXAFS spectroscopy and isotopic dilution both indicate that Zn is quite labile and mainly associated with soil organic matter in this organic-rich soil. The fact that simple organic acids were not detected in our soil, despite their presence in living plants, suggests that the bioaccumulated Zn fraction is complexed to soil organic matter after the plants' death. Thus, the persistence of Zn in the topsoil can be explained by the interdependent relationship between the soil organic matter, whose biodegradation is slowed by the high metal concentration, and Zn, which is maintained in the topsoil thanks to the overwhelming amount of soil organic matter.

Acknowledgments

We acknowledge J. L. Hazemann and O. Proux for assistance during EXAFS measurements and the ALS, the ESRF, and the LURE for the provision of beamtime. The authors thank the three anonymous reviewers for scientific advice. This research was supported by the CNRS "Programme Environnement, Vie et Société" (Grant 00N55).

Literature Cited

(1) Kabata-Pendias, A.; Pendias, H. *Trace Elements in Soils and Plants*, 3rd ed.; CRC Press: Boca Raton, FL, 2001.
(2) Godin, P.; Feinberg, M.; Ducauze, M. *Environ. Pollut.* **1985**, *10*, 97−114.
(3) Sterckeman, T.; Douay, F.; Proix, N.; Fourrier, H. *Environ. Pollut.* **2000**, *107*, 377−389.
(4) Sterckeman, T.; Douay, F.; Proix, N.; Fourrier, H.; Perdrix, E. *Water, Air Soil Pollut.* **2002**, *135*, 173−194.
(5) Gillet, S.; Ponge, J. F. *Eur. J. Soil Sci.* **2002**, *53*, 529−539.
(6) Coughtrey, P.; Jones, C.; Martin, M.; Shales, S. *Oecologia* **1979**, *39*, 51−60.
(7) Balabane, M.; Faivre, D.; Van-Oort, F.; Dahmani-Muller, H. *Environ. Pollut.* **1999**, *105*, 45−54 (and references therein).
(8) Scheinost, A.; Kretzschmar, R.; Pfister, S. *Environ. Sci. Technol.* **2002**, *36*, 5021−5028.
(9) Boyd, R. S. In *Plants That Hyperaccumulate Heavy Metals*; Brooks, R. R., Ed.; CAB International: New York, 1998; pp 181−201.
(10) Boyd, R. S.; Jaffré, T. *S. Afr. J. Sci.* **2001**, *97*.
(11) Vazquez, M. D.; Barcelo, J.; Poschenrieder, C.; Madico, J.; Hatton, P.; Baker, A. J. M.; Cope, G. H. *J. Plant Physiol.* **1992**, *140*, 350−355.
(12) Neumann, D.; zur-Nieden, U. *Phytochemistry* **2001**, *56*, 685−692.
(13) Frey, B.; Keller, C.; Zierold, K.; Schulin, R. *Plant Cell Environ.* **2000**, *23*, 675−687.
(14) Hall, J. *J. Exp. Bot.* **2002**, *53*, 1−11.
(15) O'Day, P.; Carrol, S. A.; Waychunas, G. A. *Environ. Sci. Technol.* **1998**, *32*, 943−955.
(16) Manceau, A.; Lanson, B.; Schlegel, M. L.; Hargé, J. C.; Musso, M.; Eybert-Bérard, L.; Hazemann, J. L.; Chateigner, D.; Lamble, G. M. *Am. J. Sci.* **2000**, *300*, 289−343.
(17) Isaure, M. P.; Laboudigue, A.; Manceau, A.; Sarret, G.; Tiffreau, C.; Trocellier, P.; Lamble, G.; Hazemann, J. L.; Chateigner, D. *Geochim. Cosmochim. Acta* **2002**, *66*, 1549−1567.
(18) Roberts, D.; Scheinost, A.; Sparks, D. *Environ. Sci. Technol.* **2002**, *36*, 1742−1750.
(19) Juillot, F.; Morin, G.; Ildefonse, P.; Trainor, T.; Benedetti, M.; Galoisy, L.; Calas, G.; Brown, G. *Am. Miner.* **2003**, *88*, 509−526.
(20) Isaure, M. P.; Laboudigue, A.; Manceau, A.; Sarret, G.; Tiffreau, C.; Trocellier, P. *Nucl. Instr. Methods Phys. Res. B* **2001**, *181*, 598−602.
(21) Manceau, A.; Marcus, M. A.; Tamura, N. In *Applications of Synchrotron Radiation in Low-Temperature Geochemistry and Environmental Science*; Fenter, P., Rivers, M., Sturchio, N., Sutton, S., Eds.; Reviews in Mineralogy and Geochemistry 49; Mineralogical Society of America: Washington, DC, 2002; pp 341−428.
(22) Manceau, A.; Marcus, M.; Tamura, N.; Proux, O.; Geoffroy, N.; Lanson, B. *Geochim. Cosmochim. Acta* (in press).
(23) Wasserman, S. R. *J. Phys. IV* **1997**, *7*, 203−205.
(24) Ressler, T.; Wong, J.; Roos, J.; Smith, I. L. *Environ. Sci. Technol.* **2000**, *34*, 950−958.
(25) Degryse, F.; Broos, K.; Smolders, E.; Merckx, R. *Eur. J. Soil Sci.* **2003**, *54*, 149−157.
(26) Nakhone, L.; Young, S. *Environ. Pollut.* **1993**, *82*, 73−77.
(27) Smolders, E.; Brans, K.; Foldi, A.; Merckx, R. *Soil Sci. Soc. Am. J.* **1999**, *63*, 78−85.
(28) Sinaj, S.; Machler, F.; Frossard, E. *Soil Sci. Soc. Am. J.* **1999**, *63*, 1618−1625.
(29) Balesdent, J.; Pétraud, J. P.; Feller, C. *Sci. Sol* **1991**, *29*, 95−106.
(30) Sarret, G.; Saumitou-Laprade, P.; Bert, V.; Proux, O.; Hazemann, J. L.; Traverse, A.; Marcus, M. A. M.; Manceau, A. *Plant Physiol.* **2002**, *130*, 1815−1826.
(31) Frossard, E.; Condron, L. M.; Oberson, A.; Sinaj, S.; Fardeau, J. C. *J. Environ. Qual.* **2000**, *29*, 15−23.
(32) Malinowski, E. R. *Factor Analysis in Chemistry*; Wiley: New York, 1991.
(33) Sarret, G.; Manceau, A.; Hazemann, J. L.; Gomez, A.; Mench, M. *J. Phys. IV* **1997**, *7*, 799−802.
(34) Manceau, A.; Tamura, N.; Celestre, R.; MacDowell, A.; Geoffroy, N.; Sposito, G.; Padmore, H. *Environ. Sci. Technol.* **2003**, *37*, 75−80 (and references therein).
(35) Stevenson, F. J. *Humus Chemistry*, 2nd ed.; Wiley: New York, 1994.
(36) Kupper, H.; Lombi, E.; Zhao, F. J.; McGrath, S. P. *Planta* **2000**, *212*, 75−84.
(37) Zhao, F.; Lombi, E.; Breedon, T.; McGrath, S. *Plant Cell Environ.* **2000**, *23*, 507−514.
(38) Perronnet, K.; Schwartz, C.; Gerard, E.; Morel, J. L. *Plant Soil* **2000**, *227*, 257−263.
(39) Sauvé, S.; Hendershot, W.; Allen, H. *Environ. Sci. Technol.* **2000**, *34*, 1125−1131.

Received for review October 22, 2003. Revised manuscript received February 17, 2004. Accepted February 27, 2004.

ES035171T